

Joint VSP and surface seismic tomography

Serguei Lapin*, Sonja Kisin and Hua-wei Zhou, Allied Geophysical Laboratories, Department of Geosciences, University of Houston

Summary

VSP data provide depth control and increased resolution in subsurface imaging. However, VSP tomography suffers from problems of non-uniqueness due to lack of ray crossing. In order to resolve this problem, we suggest simultaneous use of VSP and surface seismic data. We used tomographic method, which relies on the shortest path ray tracing in blocky parameterized model. The analogue of the conjugate gradient method was implemented for the inversion.

Introduction

One of the major efforts of the Allied Geophysical Laboratories of the University of Houston is the development and calibration of 3D vector imaging techniques for VSP data from Vinton Dome, onshore oil field in southwestern Louisiana. VSP data provide depth control of seismic events and resolution that is higher than the one of surface seismic data. On the other hand, VSP data are characterized by the lack of crossing of raypaths, which introduces non-uniqueness and instability in traveltome tomography. In order to increase level of ray crossing, we suggest simultaneous implementation of seismic tomography for surface seismic and VSP data.

Three-dimensional surface seismic data and 3D-3C VSP data were collected in Vinton Dome simultaneously by OPEX during survey in 1998. Surface seismic data were recorded by a radial receiver grid, and the VSP data were recorded by multilevel downhole three-component arrays located in the well G-23 (Fig. 1). Surface seismic receiver lines were radially directed away from the piercement dome. Long and short lines segments were design to alternate with spacing of 5° (Constance et al, 1999). Receivers spacing was 165 feet along a receiver line. Source locations are approximate concentric circles, with shot spacing of 165m along the arc. VSP dataset was recorded together with northern half (Fig. 1) of the surface seismic survey (Constance et al, 1999). The well G-23 had 80 three-component geophones permanently cemented in the well wall with 50 feet increments, within a depth range from 943 to 4893 feet. However, the bottom 18 levels were damaged during deployment and they were not operational for recording. The active depth range was 943 to 3993 feet.

In this abstract we will illustrate methodology applied for tomographic velocity model building and the potential of simultaneous use of VSP and surface seismic data.

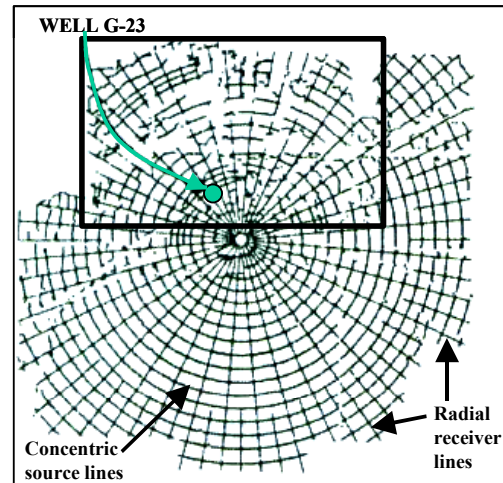


Fig.1. Acquisition map of Vinton Dome (Modified from Constance, 1999). Thick rectangular indicates source area used for VSP acquisition.

Methodology

Model partition and mesh generation

Model is partitioned into a finite number of basic model cells in our approach. We require that cells have constant seismic properties, such as wave velocity and density. In order to keep convexity of each basic cell for ray tracing, we require model interfaces to be piecewise planar. Therefore, good choices for the model cell are trapezoids in two dimensions and triangular prisms in three dimensions. The model interfaces are straight lines in 2D and planar facets in 3D. Each model cell is bounded by model vertical lines in 2D or vertical planes in 3D (Fig. 2). The parallelness of model vertical lines guarantees convexity. We keep horizontal spacing between the vertical lines constant for simplicity, but let vertical spacing between the model interfaces to vary. This allows us to follow the irregularity of the initial model interface. The triangular nature of horizontal surfaces of the model cells in three dimensions also allow us to move interfaces (i.e. one, two, or all three corner nodes) up or down without bending them. After we divide the initial model into a subset of model cells, we generate a semi-regular mesh (set of nodes) over the surfaces of each cell. Then, using the analogue of

Joint VSP and surface seismic tomography

the array of pointers we construct correspondence between the cell number and the node global number.

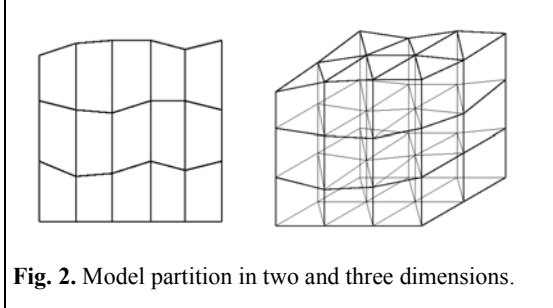


Fig. 2. Model partition in two and three dimensions.

Shortest path ray-tracing

We use the shortest path ray tracing based on an approach proposed by Moser (1991). This approach relies on graph theory in general and the theory of shortest paths in networks in particular. Shortest paths algorithms are of a discrete nature: there are a finite number of objects, and the solution to the problem can be found in a finite number of steps. The shortest path method allows to calculate all the shortest paths from one point simultaneously because calculating one path costs as much as calculating all the paths. Another advantage of shortest path algorithms is that there is no dependence on the dimension of space.

Let us use the following notation to describe briefly the shortest path algorithms. $G(N, E)$ is a graph, that is the set N of n nodes together with a set of edges E , each edge being a set of two nodes from N . A network (or weighted graph) (G, D) is a graph with a weight function D , which assigns real number (weight) to each edge E , D is a matrix with components d_{ij} . The network representing a velocity model is sparse: each node is connected only to nodes inside the same model cell. The traveltime along a path from one cell to another is defined as sum of the weights connections of the path. The shortest path from the source to all other nodes form the so-called shortest path tree, with its root at the source and the branches connecting to the other nodes. The traveltime along the shortest path from source node s to node i is denoted by t_i and obeys the Bellman's equation:

$$t_i = \min_{i \neq j} [t_j + d_{ij}] \quad i, j \in N,$$

with the initial condition

$$t(s) = 0.$$

The traveltime to node i is a minimum of the traveltimes to neighboring nodes j plus the weight of the connection.

One of the most well known shortest path algorithms is the so-called Dijkstra's algorithm (1959), which lets us find the shortest paths after exactly n iterations. The number of operations required for classical Dijkstra's algorithm to compute shortest paths is $O(n^2)$. In our work, we use a modification of Dijkstra's algorithm, which uses binary heap structure as a priority queue to store nodes. This approach helps to decrease number of operations, which is equal to $O(n \log n)$.

The ray tracing algorithm is organized as follows:

- Find the shortest (traveltime) path from one source to all predefined nodes
- For each receiver find the closest node (in the sense of traveltime), and from that node we already have shortest path to source

Repeating the above for every source give us shortest travel time paths for all pairs source/receiver.

The shortest path algorithm gives us quite accurate approximation of traveltimes if mesh is fine enough.

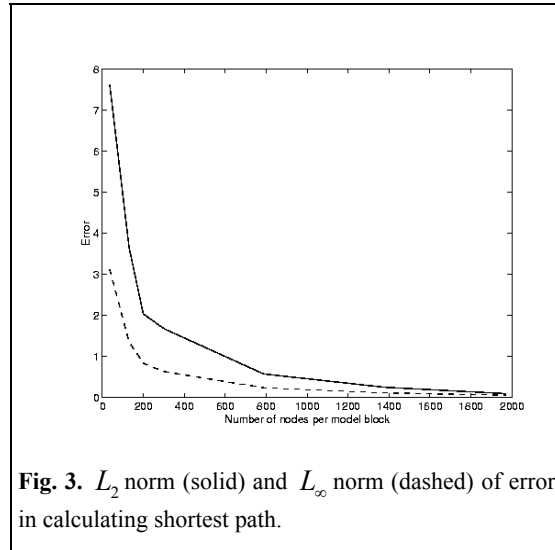


Fig. 3. L_2 norm (solid) and L_∞ norm (dashed) of error in calculating shortest path.

Inversion

The travel time of the ray passing through the model parameterized as described above depends on slowness as well as on the geometry of the model cells. If we define

Joint VSP and surface seismic tomography

$t_i(s, z)$ to be a traveltimes of the i 'th ray and $l_i(z)$ its length, then we have

$$t_i = \int_{l_i} s dl_i(z). \quad (1)$$

Applying partial differentiation with respect to s and z and approximating integrals we get

$$dt_i = \sum_l \ker_{s_{il}} ds_l + \sum_k \ker_{z_{ik}} dz_k, \quad (2)$$

where L is the number of model cells; K is the total number of interface nodes. Equation (2) can be presented in the matrix form

$$J dm = dt. \quad (3)$$

Here J is the Jacobian matrix, dm is model perturbation and dt is traveltime perturbation. Matrix J is usually nonrectangular and poorly conditioned. In order to solve (invert) (3) we use LSQR algorithm (Paige, Saunders, 1982).

Preliminary results

We constructed synthetic models for the upper sedimentary portion of the Vinton Dome area (Fig. 4). The subsurface model consists of 6 dipping layers, with velocity values of 1.9 to 3.0 km/s (Fig. 4a). The initial model (Fig. 4b) was a layer-cake model of subsurface. Ray coverage of VSP data was rather poor (Fig. 4c) and provided the update of the velocity model only in the limited subsurface area (Fig. 4d). For the same subsurface model, we introduced only 6 additional surface receivers (Fig. 4e). The ray coverage and ray crossing has been significantly increased, even with introduction of such a limited number of receivers. The final tomographic model (Fig. 4f) completely corresponds to the real one (Fig. 4a), showing that joint VSP and surface seismic tomography significantly improves our ability to recover subsurface structure.

Conclusions

Our tomographic approach proved to be efficient and accurate. Joint usage of VSP and surface data significantly improves the definition of the subsurface structure.

References

Constance, P.A. et al., 1999, Simultaneous acquisition of 3-D surface seismic data and 3-C, 3-D VSP data, 69th Ann. Internat. Mtg: Soc. of Expl. Geophys. Expanded Abstracts, 104-107.
Dijkstra E.W., 1959, A note on two problems in connexion with graphs: *Numerische Mathematik*, **1**, 269 – 271.

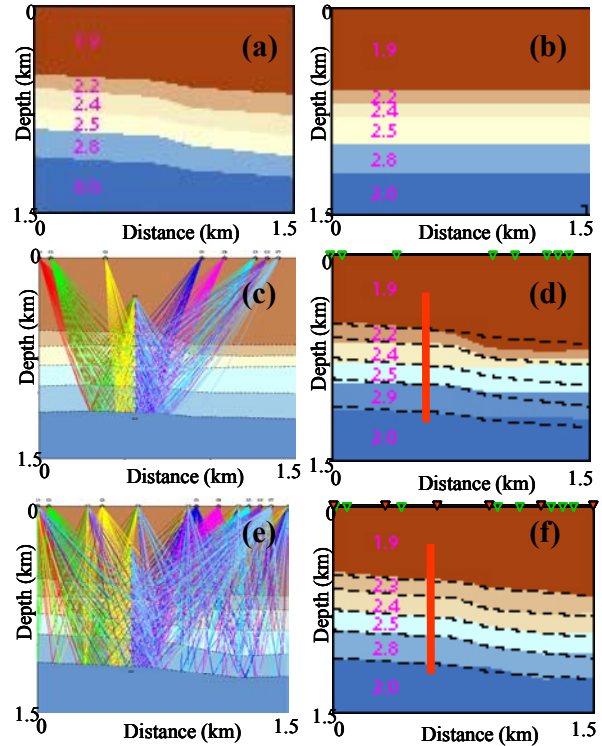


Fig. 4. Comparison between VSP tomography and joint VSP and surface tomography. (a) True subsurface model, (b) Initial subsurface model, (c) VSP ray tracing in the true model, (d) Tomographic result after 5 iterations using only VSP data, (e) Ray tracing using both VSP and surface receivers, (f) Tomographic results after 5 iterations using joint VSP and surface seismic tomography. Green triangles indicate positions of seismic sources, red line position of 60 VSP receivers and red triangles position of surface receivers.

Moser, T.J., 1991, Shortest path calculation of seismic rays: *Geophysics*, **56**, 59 – 67.

Paige C.C., Saunders M.A., 1982, LSQR: An algorithm for sparse linear equations and sparse least squares: *ACM Trans. On Math. Software*, **8**, 43-71.

Zhou, H., 1997b, Determination of velocities and interfaces by multi-scale tomography: 67th Ann. Internat. Mtg: Soc. of Expl. Geophys. Expanded Abstracts, 1877-1880.

Acknowledgements

Authors would like to thank OPEX for providing data and sponsors of Allied Geophysical Laboratories.